Research Paper

On

Variational Doppler radar analysis system (VDRAS)

By Sahibzad Khan (Director)

Regional Meteorological Centre Lahore.

Table of Contents

Abstract:-

The purpose of the research reported in this paper is to develop a vibrational data analysis system that can be used to assimilate data from one or more Doppler radars. In the first part of this two-part study, the technique used in this analysis system is described and tested using data from a simulated warm rain convective storm. The analysis system applies the 4D vibrational data assimilation technique to a cloud-scale model with a warm rain parameterization scheme. The 3D wind, thermodynamically, and microphysical fields are determined by minimizing a cost function, defined by the difference between both radar observed radial velocities and reflectivities (or rainwater mixing ratio) and their model predictions. The ad joint of the numerical model is used to provide the sensitivity of the cost function with respect to the control variables.

Experiments using data from a simulated convective storm demonstrated that the vibrational analysis system is able to retrieve the detailed structure of wind, thermodynamics, and microphysics using either dual-Doppler or single-Doppler information. However, less accurate velocity fields are obtained when single-Doppler data were used. In both cases, retrieving the temperature field is more difficult than the retrieval of the other fields. Results also show that assimilating the rainwater mixing ratio obtained from the reflectivity data results in a better performance of the retrieval procedure than directly assimilating the reflectivity. It is also found that the system is robust to variations in the $Z–q_r$ relation, but the microphysical retrieval is quite sensitive to parameters in the warm rain scheme. The technique is robust to random errors in radial velocity and calibration errors in reflectivity.

Main Purpose :-

The main purpose of this paper is to describe the new variational Doppler radar analysis system and demonstrate its ability in retrieving the 3D wind, thermodynamical, and microphysical structure of convective storms. Issues associated with the adjoint of moist processes will also be discussed. We test the retrieval technique on simulated data of moist convection initiated from a warm, moist bubble.

Section1:-

Section 1 is the basic introduction of variational Doppler radars.

Section 2:-

This section describes the numerical model and the physical parameterization schemes. The variational data assimilation technique used in VDRAS will be described

Section 3:-

Some special treatments of the moist processes in the ad joint model will also be addressed in this section.

Section 4:-

The control simulation is described and the results of retrieval experiments are presented.

Section 5:-

Summary and discussion are given in the last section.

Section1:-

Introduction:-

During the past few decades, observations from Doppler radars have been widely used in diagnostic studies of convective systems, severe weather detection, and short-term forecasting. With the deployment of the NEXRAD network in the 1990s, there has been an increased interest in the possibility of operational cloud-scale numerical forecasting. One of the major challenges in cloud-scale numerical weather prediction is obtaining accurate initial conditions. Doppler radars, which provide observations of radial velocity and reflectivity with a spatial resolution of a few hundred meters every 3–10 min, are practically the only instrument capable of sampling the four-dimensional structure of storm-scale flows. To specify the state of the atmosphere using these data, it is necessary to develop techniques to derive detailed meteorological fields that are not directly measured by Doppler radars. The quantitative information obtained thereby will not only provide initial conditions for cloud-scale numerical models but also help improve operational forecasting skills and enhance our understanding of precipitating weather systems.

fields can then be obtained with the aid of the equations of motionOver the past few decades, various methods have been developed to infer detailed information from single or multiple-Doppler observations. Using observations from a single-Doppler radar, it has been shown that the boundary layer flow can be retrieved with reasonable accuracy .With the availability of multiple-Doppler radars, researchers have demonstrated that the three-dimensional wind field can be derived through the use of the mass continuity equation and the thermodynamic. Methods to diagnose microphysical variables from radar data have also been examined by a number of researchers.A cloud model contains parameterized moist processes that are often characterized by on/off switches. These processes are often highly nonlinear and discontinuous. Since the adjoint model was initially derived for differentiable systems of equations, a model with discontinuous moist processes may present some problems. Recently, as more and more researchers have begun to include physical parameterization processes in their 4DVAR systems, the problems related to on/off switches have drawn attention in the data assimilation community.

1.1Weather Radar Observations

The Global Observing System (GOS) is made up of many component observing systems which contribute observations of meteorological parameters in support of the World Weather Watch (WWW) Programmed and fall under the two major categories, namely Surface-based Observations and Space-based Observations.In addition to the better known and more traditional systems that provide *in situ* observations at both the earth's surface and through the troposphere and lower stratosphere (Synoptic, Marine and Aircraft-based Observations), there is a relatively new suite of observing systems that can be utilized to derive observations through remote sensing technologies and techniques.Within the category of surface-based remote sensingsystems is the weather radar observing system, from which Weather Radar Observationsare provided to the WWW Programmed.

1.2Weather Radar Observations

Weather radars have been used in the detection of precipitating water droplets and the derivation of rainfall rates within clouds (Cumulonimbus and Nimbostratus) since the 1950s.Most modern weather radars utilize a pulse-Doppler technique that, in addition to providing estimates of precipitation rate, also enable the detection of droplet motion with respect to the radar and, as a result, can be used to determine radial wind speeds. More recently, dual polarized weather radars have been developed that enable more accurate determination of precipitation types and sizes.

1.3WSR & Doppler radars

Weather radar, also called weather surveillance radar (WSR) and Doppler weather radar, is a type of radar used to locate precipitation, calculate its motion, and estimate its type (rain, snow, hail etc.). Modern weather radars are mostly pulse-Doppler radars, capable of detecting the motion of rain droplets in addition to the intensity of the precipitation. Both types of data can be analyzed to determine the structure of storms and their potential to cause severe weather. During World War II, radar operators discovered that weather was causing echoes on their screen, masking potential enemy targets. Techniques were developed to filter them, but scientists began to study the phenomenon. Soon after the war, surplus radars were used to detect precipitation. Since then, weather radar has evolved on its own and is now used by national weather services, research departments in universities, and in television newscasts. Raw images are routinely used and specialized software can take radar data to make short term forecasts of future positions and intensities of rain, snow, hail, and other weather phenomena. Radar output is even incorporated into numerical weather prediction models to improve analyses and forecasts.

1.4How a weather radar works

Sending radar pulses

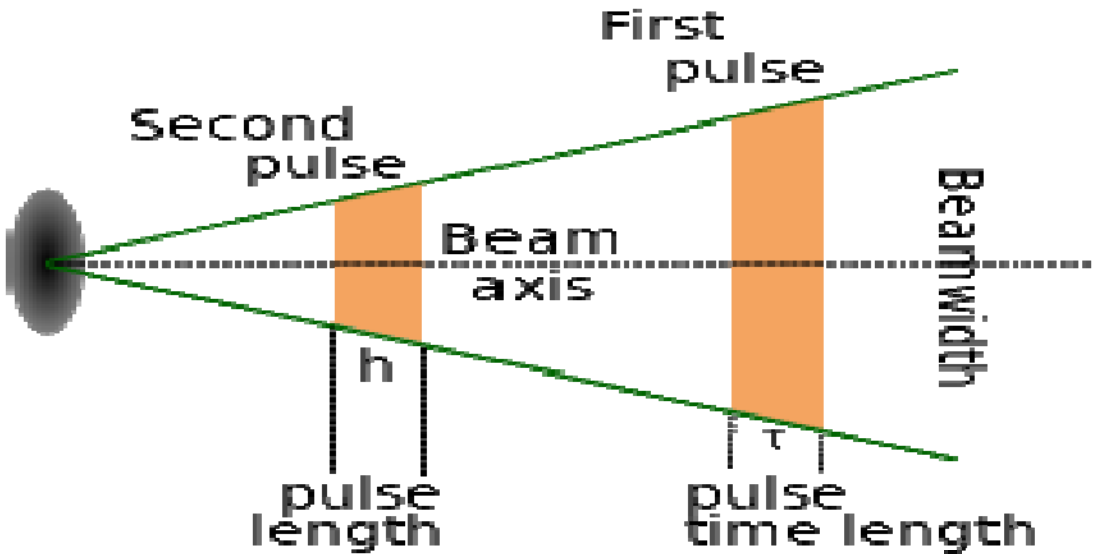

A radar beam spreads out as it moves away from the radar station, covering an increasingly large volume.

Weather radars send directional pulses of microwave radiation, on the order of a microsecond long, using a cavity magnetron or klystron tube connected by a waveguide to a parabolic antenna. The wavelengths of 1 – 10 cm are approximately ten times the diameter of the droplets or ice particles of interest, because Rayleigh scattering occurs at these frequencies. This means that part of the energy of each pulse will bounce off these small particles, back in the direction of the radar station. Shorter wavelengths are useful for smaller particles, but the signal is more quickly attenuated. Thus 10 cm (S-band) radar is preferred but is more expensive than a 5 cm C-band system. 3 cm X-band radar is used only for short-range units, and 1 cm K-band weather radar is used only for research on small-particle phenomena such as drizzle and fog. Radar pulses spread out as they move away from the radar station. Thus the volume of air that a radar pulse is traversing is larger for areas farther away from the station, and smaller for nearby areas, decreasing resolution at far distances. At the end of a 150 – 200 km sounding range, the volume of air scanned by a single pulse might be on the order of a cubic kilometer. This is called the pulse volume. The volume of air that a given pulse takes up at any point in time may be approximated by the formula $v = hr^2\theta^2$, where v is the volume enclosed by the pulse, h is pulse width (in e.g. meters, calculated from the duration in seconds of the pulse times the speed of light), r is the distance from the radar that the pulse has already traveled (in e.g. meters), and θ is the beam width (in radians). This formula assumes the beam is symmetrically circular; "r" is much greater than "h" so "r" taken at the beginning or at the end of the pulse is almost the same.

1.5Listening for return signals

Between each pulse, the radar station serves as a receiver as it listens for return signals from particles in the air. The duration of the "listen" cycle is on the order of a millisecond, which is a thousand times longer than the pulse duration. The length of this phase is determined by the need for the microwave radiation (which travels at the speed of light) to propagate from the detector to the weather target and back again, a distance which could be several hundred kilometers. The horizontal distance from station to target is calculated simply from the amount of time that lapses from the initiation of the pulse to the detection of the return signal. The time is converted into distance by multiplying by the speed of light in air:

$$\text{Distance} = c\frac{\Delta t}{2n},$$

where$c$ = 299,792.458 km/s is the speed of light, and $n \approx 1.0003$ is the refractive index of air. If pulses are emitted too frequently, the returns from one pulse will be confused with the returns from previous pulses, resulting in incorrect distance calculations.

1.6Determining height

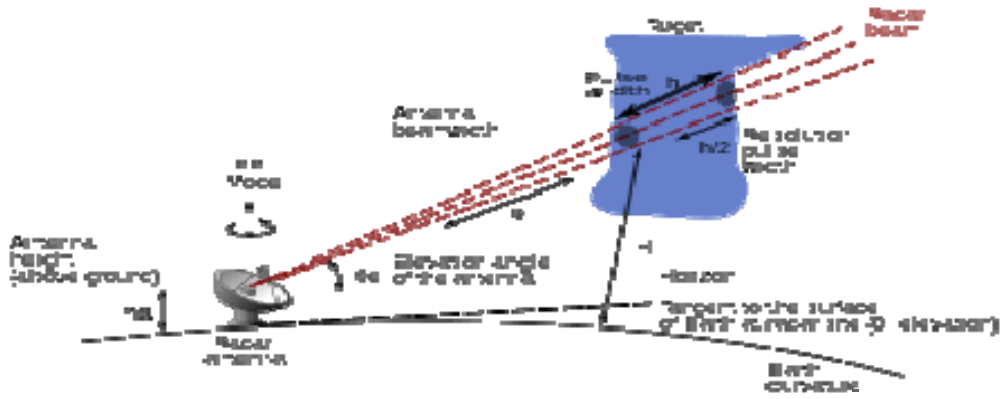

The radar beam path with height

Assuming the Earth is round, the radar beam in vacuum would rise according to the reverse curvature of the Earth. However, the atmosphere has a refractive index that diminishes with height, due to its diminishing density. This bends the radar beam slightly toward the ground and with a standard atmosphere this is equivalent to considering that the curvature of the beam is 4/3 the actual curvature of the Earth. Depending on the elevation angle of the antenna and other considerations, the following formula may be used to calculate the target's height above ground:

$$H = \sqrt{r^2 + (k_e a_e)^2 + 2rk_e a_e \sin(\theta_e)} - k_e a_e + h_a,$$

Where:

r = distance radar–target,

k_e = 4/3,

a_e = Earth radius,

ϑ_e = elevation angle above the radar horizon,

h_a = height of the feedhorn above ground

A weather radar network uses a series of typical angles that will be set according to the needs. After each scanning rotation, the antenna elevation is changed for the next sounding. This scenario will be repeated on many angles to scan all the volume of air around the radar within the maximum range. Usually, this scanning strategy is completed within 5 to 10 minutes to have data within 15 km above ground and 250 km distance of the radar. For instance in Canada, the 5 cm weather radars use angles ranging from 0.3 to 25 degrees. The image to the right shows the volume scanned when multiple angles are used. Due to the Earth's curvature and change of index of refraction with height, the radar cannot "see" below the height above ground of the minimal angle closer to the radar than the maximal one (shown as a red cone in the center).

1.7Calibrating intensity of return:-

Because the targets are not unique in each volume, the radar equation has to be developed beyond the basic one.

$$P_r = \left[P_t \frac{G^2 \lambda^2 \sigma_0}{(4\pi)^3 R^4}\right] \propto \frac{\sigma_0}{R^4}$$

where P_r is received power, P_t is transmitted power, G_t is the gain of the transmitting antenna, λ is radar wavelength, σ is the radar cross section of the target and R is the distance from transmitter to target.

In this case, we have to add the cross sections of all the targets:

$$\sigma_0 = \bar{\sigma}_0 = V \sum \sigma_{0i} = V\eta$$

$$\begin{cases} V & = \text{scanned volume} \\ & = \text{pulse length } X \text{ beam width} \\ & = \left[\frac{cT}{2}\right]\left[\frac{\pi R^2\theta^2}{4}\right] \end{cases}$$

Where c is the light speed, T is temporal duration of a pulse and θ is the beam width in radians.

In combining the two equations:

$$P_r = \left[P_t \frac{G^2\lambda^2}{(4\pi)^3 R^4}\right]\left[\frac{cT}{2}\right]\left[\frac{\pi R^2\theta^2}{4}\right]\eta = \left[P_t T G^2 \lambda^2 \theta^2\right]\left[\frac{c}{512(\pi^2)}\right]\frac{\eta}{R^2}$$

$$P_r \propto \frac{\eta}{R^2}$$

Notice that the return now varies inversely to R^2 instead of R^4. In order to compare the data coming from different distances from the radar, one has to normalize them with this ratio.

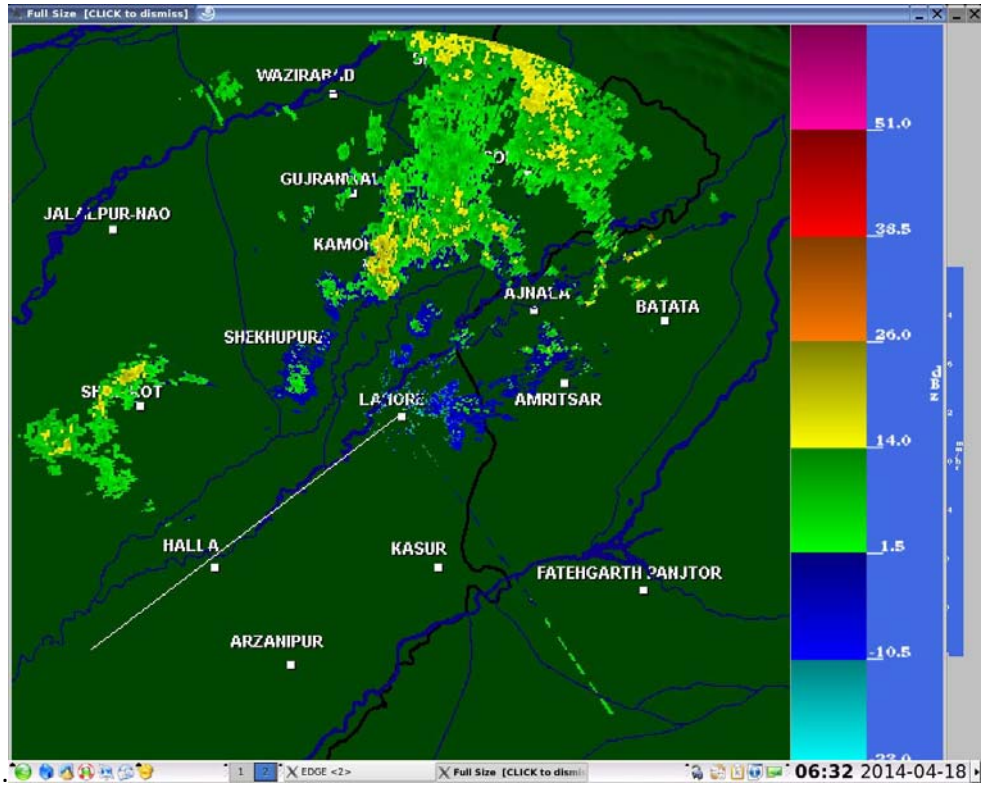

Image of Doppler radar for intensity calibration installed by Pakistan Meteorological Department at Lahore (Pakistan).

1.8How to read reflectivity on a radar display

Radar returns are usually described by color or level. The colors in a radar image normally range from blue or green for weak returns, to red or magenta for very strong returns. The numbers in a verbal report increase with the severity of the returns. For example, the U.S. National Doppler Radar sites use the following scale for different levels of reflectivity:

- magenta: 65 dBZ (extremely heavy precipitation, possible hail)
- red: 52 dBZ
- yellow: 36 dBZ
- green: 20 dBZ (light precipitation)

Strong returns (red or magenta) may indicate not only heavy rain but also thunderstorms, hail, strong winds, or tornadoes, but they need to be interpreted carefully, for reasons described below.

1.9Aviation conventions

When describing weather radar returns, pilots, dispatchers, and air traffic controllers will typically refer to three return levels.

- **level 1** corresponds to a green radar return, indicating usually light precipitation and little to no turbulence, leading to a possibility of reduced visibility.
- **level 2** corresponds to a yellow radar return, indicating moderate precipitation, leading to the possibility of very low visibility, moderate turbulence and an uncomfortable ride for aircraft passengers.
- **level 3** corresponds to a red radar return, indicating heavy precipitation, leading to the possibility of thunderstorms and severe turbulence and structural damage to the aircraft.

1.10Precipitation types:-

Some displays provided by commercial weather sites, like The Weather Channel or *Intellcast*, show precipitation types during the winter month : rain, snow, mixed precipitations (sleet and freezing rain). This is not an analysis of the radar data itself but a post-treatment done with other data sources, the primary being surface reports (METAR).[21]

Over the area covered by radar echoes, a program assigns a precipitation type according to the surface temperature and dew point reported at the underlying weather stations. Precipitation types reported by human operated stations and certain automatic ones (AWOS) will have higher weight.[22] Then the program does interpolations to produce an image with defined zones. These will include interpolation errors due to the calculation. Mesoscale variations of the precipitation zones will also be lost.[21] More sophisticated programs use the numerical weather prediction output from models, such as NAM and WRF, for the precipitation types and apply it as a first guess to the

radar echoes, then use the surface data for final output.

Until dual-polarization (section Polarization below) data are widely available, any precipitation types on radar images are only indirect information and must be taken with care.

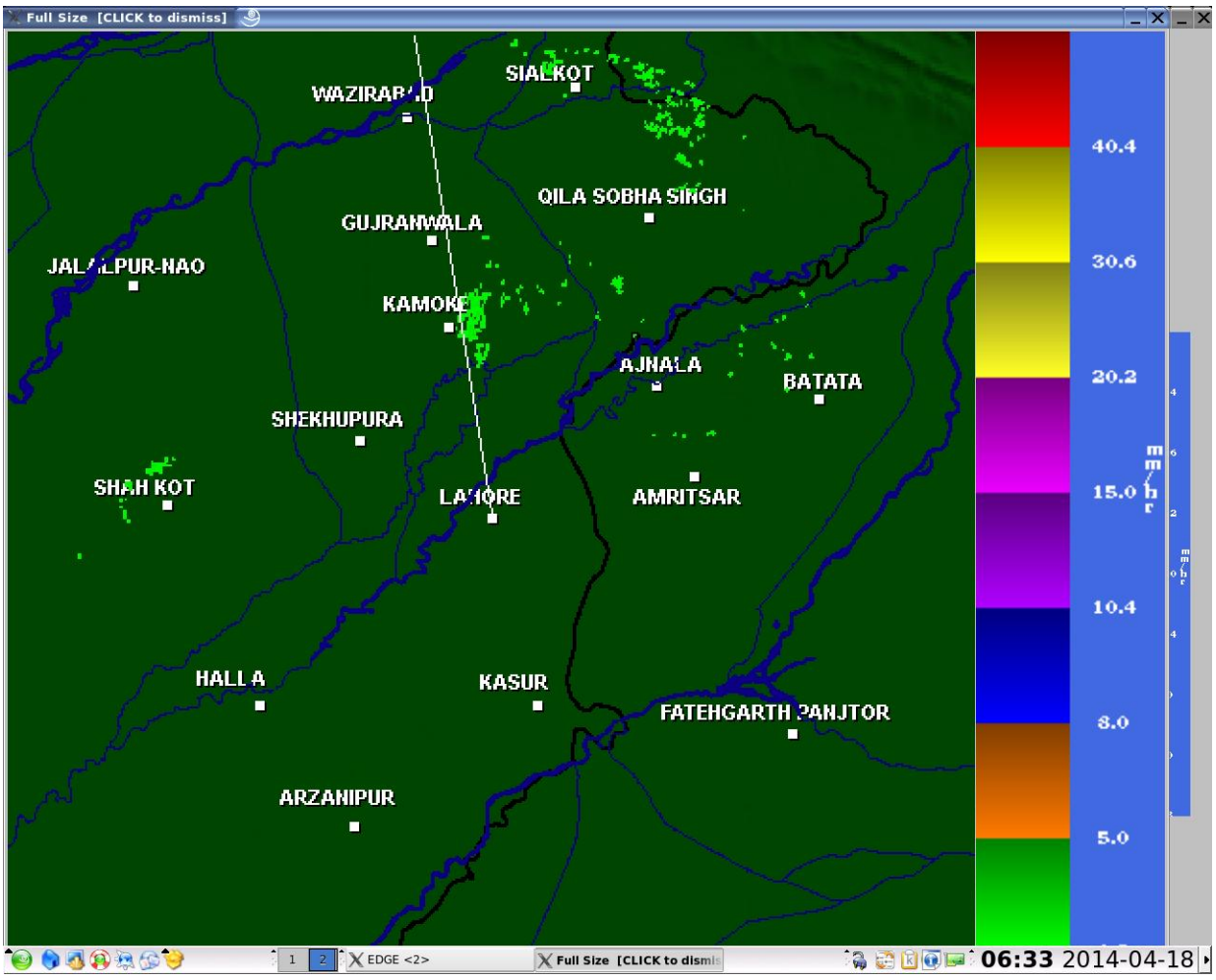

Image of Doppler radar for precipitation calibration installed by Pakistan Meteorological Department at Lahore (Pakistan).

1.11Pulse pair

Doppler weather radars use this phase difference (pulse pair difference) to calculate the precipitation's motion. The intensity of the successively returning pulse from the same scanned volume where targets have slightly moved is:

$$I = I_0 \sin\left(\frac{4\pi(x_0 + v\Delta t)}{\lambda}\right) = I_0 \sin(\Theta_0 + \Delta\Theta)$$

$$\begin{cases} x = \text{distance from radar to target} \\ \lambda - \text{radar wavelength} \\ \Delta t = \text{time between two pulses} \end{cases}$$

So $\Delta\Theta = \frac{4\pi v \Delta t}{\lambda}$, v = target speed = $\frac{\lambda \Delta\Theta}{4\pi\Delta t}$. This speed is called the radial Doppler velocity because it gives only the radial variation of distance versus time between the radar and the target. The real speed and direction of motion has to be extracted by the process described below.

1.12Doppler interpretation

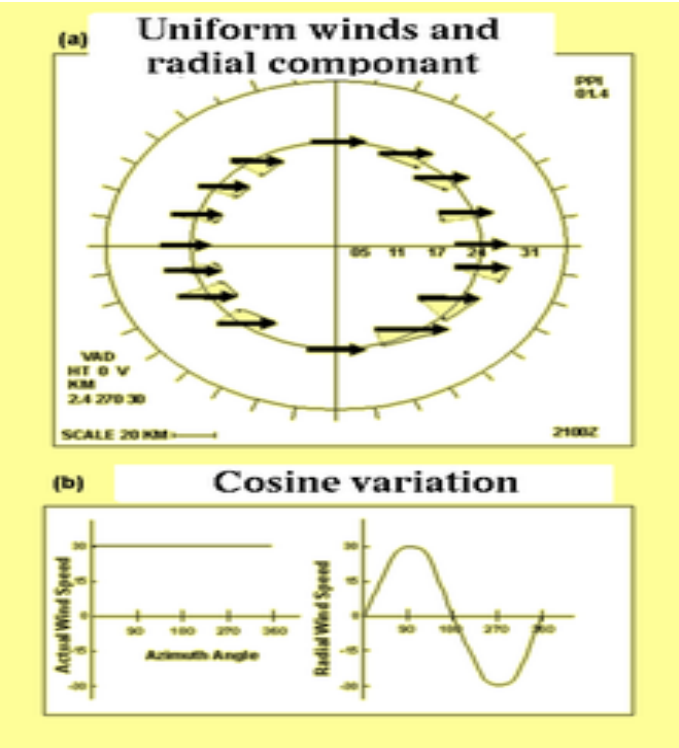

Radial component of real winds when scanning through 360 degrees

In a uniform rainstorm moving eastward, a radar beam pointing west will "see" the raindrops moving toward itself, while a beam pointing east will "see" the drops moving away. When the beam scans to the north or to the south, no relative motion is noted.

1.13Polarization:-

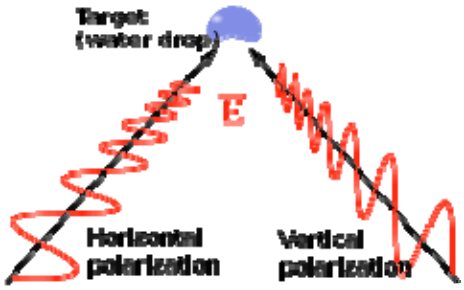

Targeting with dual-polarization will reveal the form of the droplet.

Droplets of falling liquid water tend to have a larger horizontal axis due to the drag coefficient of air while falling (water droplets). This causes the water moleculedipole to be oriented in that direction; so, radar beams are, generally, polarized horizontally in order to receive the maximal signal reflection.

If two pulses are sent simultaneously with orthogonal polarization (vertical and horizontal, Z_V and Z_H respectively), two independent sets of data will be received. These signals can be compared in several useful ways:

- Differential Reflectivity (Z_{dr}) – The differential reflectivity is the ratio of the reflected vertical and horizontal power returns as Z_V/Z_H. Among other things, it is a good indicator of drop shape and drop shape is a good estimate of average drop size.
- Correlation Coefficient (ρ_{hv}) – A statistical correlation between the reflected horizontal and vertical power returns. High values, near one, indicate homogeneous precipitation types, while lower values indicate regions of mixed precipitation types, such as rain and snow, or hail.
- Linear Depolarization Ratio (*LDR*) – This is a ratio of a vertical power return from a horizontal pulse or a horizontal power return from a vertical pulse. It can also indicate regions where there is a mixture of precipitation types.
- Specific Differential Phase (θ_{dp}) – The specific differential phase is a comparison of the returned phase difference between the horizontal and vertical pulses. This change in phase is caused by the difference in the number of wave cycles (or wavelengths) along the propagation path for horizontal and vertically polarized waves. It should not be confused with the Doppler frequency shift, which is caused by the motion of the cloud and precipitation particles. Unlike the differential reflectivity, correlation coefficient and linear depolarization ratio, which are all dependent on reflected power, the specific differential phase is a "propagation effect." It is a very good estimator of rain rate and is not affected by attenuation.

With more information about particle shape, dual-polarization radars can more easily distinguish airborne debris from precipitation, making it easier to locate tornados.

Section 2:-

Numerical model:-

2.1 Basic equations

The model contains six prognostic equations. They are the three momentum equations, the thermodynamic equation, the rainwater equation, and the total water equation. Using the an elastic approximation, the momentum equations are written as

$$\frac{d\bar{\rho}u}{dt} = -\frac{\partial p'}{\partial x} + \nu\nabla^2\bar{\rho}u, \qquad (2.1)$$

$$\frac{d\bar{\rho}v}{dt} = -\frac{\partial p'}{\partial y} + \nu\nabla^2\bar{\rho}v, \qquad (2.2)$$

$$\frac{d\bar{\rho}w}{dt} = -\frac{\partial p'}{\partial z} + g\bar{\rho}\left(\frac{T'}{T} + 0.61q_v' - q_c - q_r\right) + \nu\nabla^2\bar{\rho}w. \qquad (2.3)$$

The mass continuity equation is written as

$$\frac{\partial\bar{\rho}u}{dx} + \frac{\partial\bar{\rho}v}{dy} + \frac{\partial\bar{\rho}w}{dz} = 0. \qquad (2.4)$$

Here, u,v, and w are the wind velocities and q_v, q_c, and q_r are mixing ratios for water vapor, cloud water, and rain water, respectively; T, ρ, and p are the temperature, the density of air, and the pressure, respectively. The primed variables represent the deviations from the initial unperturbed state whose variables are denoted withoverbars. The quantity ν is the eddy viscosity. The perturbation pressure p' is a diagnostic variable that can be obtained by solving the Poisson equation

$$\nabla^2 p' = -\nabla\cdot(\mathbf{v}\cdot\nabla\bar{\rho}\mathbf{v}) + g\bar{\rho}\frac{\partial}{\partial z}\left(\frac{T'}{T} + 0.61q_v' - q_c - q_r\right). \qquad (2.5)$$

The thermodynamic equation is written in terms of liquid water potential temperature, θ_l, following Tripoli and Cotton (1981):

$$\frac{d\bar{\rho}\theta_l}{dt} = -\frac{L_v\bar{\rho}}{c_p T}\frac{\theta_l^2}{\theta}\frac{dV_{Tm}q_r}{dz} + \kappa\nabla^2\bar{\rho}\theta_l. \qquad (2.6)$$

The variable V_{Tm} is the mass-weighted terminal velocity, which will be described later. The quantity κ is the diffusivity of liquid water potential temperature and L_v is the latent heat of vaporization. The liquid water potential temperature is a conserved quantity with respect to condensation and evaporation. It is defined by

$$\theta_l = \theta\left(1 - \frac{L_v}{c_p T}(q_c + q_r)\right). \qquad (2.7)$$

The equations governing the rainwater q_r and total water content q_t are

$$\frac{d\bar{\rho}q_r}{dt} = R_c + R_a + R_e + \bar{\rho}\frac{dV_{\mathrm{Tm}}q_r}{dz} + \kappa\nabla^2\bar{\rho}q_r, \qquad (2.8)$$

$$\frac{d\bar{\rho}q_t}{dt} = \bar{\rho}\frac{dV_{\mathrm{Tm}}q_r}{dz} + \kappa\nabla^2\bar{\rho}q_t. \qquad (2.9)$$

Here, R_a is the transfer rate from cloud water to rainwater due to auto conversion, R_c is the transfer rate from cloud water to rainwater due to accretion, and R_e is the evaporation rate resulting from the evaporation of raindrops in sub saturated air. The parameterization of these three quantities will be given later. The total water content q_t is defined by

$$q_t = \begin{cases} q_c + q_{vs} + q_r, & \text{if } (q_v \geq q_{vs}) \\ q_v + q_r, & \text{if } (q_v < q_{vs}). \end{cases} \qquad (2.10)$$

The temperature and cloud water mixing ratios are diagnosed from the prognostic variables by assuming that all vapor in excess of the saturation value is converted to cloud water. These variables are related through

$$T = \left(\frac{p}{p_0}\right)^{R/c_p}\theta_l\left(1 + \frac{l_v}{c_p T}(q_c + q_r)\right), \qquad (2.11)$$

and

$$q_c = \begin{cases} (q_t - q_{vs} - q_r), & \text{if } (q_v \geq q_{vs}) \\ 0, & \text{if } (q_v < q_{vs}), \end{cases} \qquad (2.12)$$

whereq_{vs} is the saturation mixing ratio given by

$$q_{vs} = \frac{3.8}{p}\exp\left(17.27\frac{T - 273.16}{T - 35.86}\right). \qquad (2.13)$$

A bisection iteration scheme is used to obtain the temperature from Eqs. (2.11), (2.12), and (2.13). The temperature is computed within 0.01°C accuracy, which generally takes less than 10 iterations.

In this model, the liquid water potential temperature is chosen as the thermodynamically variable so that only two prognostic equations are required for the microphysics (q_r and q_t). As will be seen in the following section, the number of control variables of the optimization problem depends on the number of prognostic variables in the model. A model system with two microphysical prognostic equations will obviously reduce the number of control variables

compared to a model system that requires three microphysical prognostic equations (e.g., q_c, q_r, and q_v).

All the model variables are scaled by their typical values and the numerical model is coded in terms of dimensionless variables. The reason for doing this is to balance the magnitude of the different variables such that each variable has a similar weight during the optimization, and hence a better convergence rate.

2.2. **Physical processes**

The physical processes allowed in this model are condensation and evaporation of cloud water (implicit in θ_l), evaporation of raindrops in subsaturated air, autoconversion of cloud to rain, accretion of cloud by rain, and sedimentation of rain.

Autoconversion and evaporation of rain are parameterized

$$R_a = \begin{cases} \alpha(q_c - q_{\text{crit}}), & \text{for } q_c > q_{\text{crit}} \\ 0, & \text{for } q_c < q_{\text{crit}}, \end{cases} \qquad (2.14)$$

$$R_e = \beta(q_v - q_{vs})(\rho q_r)^{0.65}, \qquad (2.15)$$

The quantity a is a correction factor defined by $a=(p_0/\bar{p})^{0.4}$, where $\bar{p}$ is the base-state pressure and p_0 is the pressure at the ground. The rainwater mixing ratio q_r is in units g kg^{-1}. Accretion is parameterized using the expression $R_c = \gamma q_c q^{7/8}{}_r$, (2.17) where γ is set to 0.002 s$^{-1.}$

Section 3:-

3. Description of the technique used in VDRAS
3.1 Definition of the cost function

The four-dimensional variational data assimilation technique is applied in this analysis system. The objective is to find an initial state that can, upon model integration, produce output parameters matching the observations as closely as possible. A cost function measuring the misfit between the model and data is defined in terms of the radar observed variables, that is, the radial velocity and reflectivity. Assuming that the observational errors of each field are uncorrelated in space and time, the cost function J_1 is given by

$$J_1 = \sum_{\sigma,\tau,i} [\eta_v(V_{r,i} - V^{ob}_{r,i})^2 + \eta_z(Z - Z^{ob}_i)^2] + J_b + J_p. \quad (3.1)$$

where σ represents the spatial domain and τ represents the temporal domain. The index i stands for the ith radar. The quantities $V^{ob}_{r,i}$ and Z^{ob}_i are observations of the radial velocity and reflectivity, respectively, from the ith radar. Here, $V_{r,i}$ and Z are their model. On the other hand, a set of rainwater data q^{ob}_r can be obtained from the reflectivity observations. If we take q^{ob}_r as observations, another cost function J_2 can be defined as

$$J_2 = \sum_{\sigma,\tau,i} [\eta_v(V_{r,i} - V^{ob}_{r,i})^2 + \eta_q(q_r - q^{ob}_{r,i})^2] + J_b + J_p, \quad (3.4)$$

where q_r is the model-predicted rainwater mixing ratio (units of g kg^{-1}). The radial velocity $V_{r,i}$ in both Eqs. (3.1) and (3.4) is calculated using the Cartesian velocity components (u, v, w) from the model integration through the relation

$$V_{r,i} = u\frac{x - x_i}{r_i} + v\frac{y - y_i}{r_i} + (w - V_{\mathrm{Tm}})\frac{z - z_i}{r_i}, \quad (3.5)$$

where V_{Tm} is the terminal velocity of the precipitation given by Eq. (2.16). Here, r_i is the distance between a grid point (x, y, z) and the ith radar location (x_i, y_i, z_i).

Either J_1 or J_2 can be used as the cost function in a retrieval experiment. Most experiments presented in section 4 of this paper used the cost function J_2. Experiments using J_1 as the cost function will also be discussed and compared with those using J_2.

The quantities η_v, η_z, and η_q in Eqs. (3.1) and (3.4) are weighting coefficients for radial velocity, In Eq. (3.1) and (3.4), Z^{ob}_i and $q^{ob}_{r,i}$ denote the observations of the reflectivity and rainwater mixing ratio from the ith radar.

The parameters J_b and J_p in the cost functions J_1 and J_2 represent background and penalty terms, respectively. Since radar data are concentrated only in the region where scatterers exist, there are no radar observations outside that region.. The quantity J_p in the cost function represents the spatial and temporal smoothness penalty functions.

3.2. Special treatment of the moist processes in the adjoint model

. These moist processes have two general characteristics: one is that they are associated with on/off switches; the other is that the parameterization schemes are often highly nonlinear. Since the adjoint model was originally derived for a differentiable system of equations and used to provide first-order derivative information of the cost function, moist processes with nondifferentiable on/off switches and a high degree of nonlinearity can cause difficulties in the minimization procedure. The first adjoint models with full physics were developed by keeping the on/off switches the same as in the basic state or, in other words, by ignoring the variation of the switching time caused by the perturbationUsing simple differential equations, gave rigorous mathematical derivations for physical processes that contain on/off switches.

When the rainwater mixing ratio is close to zero, both parameterization schemes yield a very large gradient with respect to the rainwater mixing ratio. This can be easily shown by taking the derivative of Eqs. (2.15) and (2.16) with respect to q_r to yield

$$\frac{\partial R_e}{\partial q_r} = 0.65\beta\rho(q_v - q_{vs})(\rho q_r)^{-0.35}, \qquad (3.7)$$

and

$$\frac{\partial V_{\mathrm{Tm}}}{\partial q_r} = 0.125 \times 5.40a(\rho q_r)^{-0.875}. \qquad (3.8)$$

Section 4:-

4. Retrieving cloud structure of a simulated storm

4.1Control simulation

The control experiment was a simulation of moist convection initiated by a warm, moist bubble. The integration domain was 33.5 km in both horizontal directions and 10 km in the vertical, with grid intervals $\Delta x = \Delta y = 500$ m and $\Delta z = 400$ m. The sounding used for the initial temperature and moisture profiles is shown by the solid linesThe initial velocity fields were assumed zero. To initiate convection, a warm, moist bubble was inserted in the center of the domain at a height of 2 km. The initial impulse was 8 km wide and 4 km deep, with a temperature excess of 1°C and moisture excess of 1 g kg^{-1}.The boundary conditions for the velocities normal to the boundaries are assumed zero and, for other variables, their derivatives normal to the boundaries are assumed zero. The eddy viscosity ν was set to 150 m^2 s^{-1}, a typical value used in numerical simulations, and κ was set to 3ν. The modifications of the parameterization schemes described in the last section were not used in the control simulation.Cloud first started to form in the model at about 17 min when the warm bubble reached the lifting condensation level (about 4 km). The storm was fully developed at about 33 min with a maximum rainwater mixing ratio of ~3 g kg^{-1} and maximum vertical velocity of ~16 m s^{-1}.. A mushroom-shaped cloud is formed and the storm is characterized by a strong central updraft. The positive temperature excess is 2.86°C. The negative temperature excess above it is caused by adiabatic cooling. In the dissipating stage of the storm.

4.2 Retrieval experiments and results

In this section, we will test the ability of VDRAS by performing a number of "identical twin" experiments. In our experiments, the "observations" of radial velocities were constructed using the Cartesian velocity components and rainwater mixing ratio in the control simulation through Eq. (3.5). The "observations" of reflectivity were derived from the rainwater mixing ratio in the control simulation using Eq. (3.2) or (3.3). In most of the experiments, we assume two radars are available. The retrieval was performed on a domain of $13 \times 13 \times 10$ km^3 with a grid spacing of 500 m in the horizontal and 400 m in the vertical. Although a Doppler radar observes reflectivity, in most of the following experiments, the rainwater mixing ratio that can be estimated using a Z–q_r relation will be used as observational data. That is, the cost function (3.4) is minimized. The problem of directly assimilating reflectivity data will be discussed in a later experiment. For practical reasons, the retrieval experiments were stopped as the cost function leveled out. This generally occurred between 50 and 100 iterations. We will show results using 100 iterations for all experiments presented in this paper. The quality of the retrieval will be assessed by the relative rms error and by comparing the retrieved fields with the actual fields at the end of the assimilation window. The relative rms error is the rms error normalized by the standard deviation of the actual field.

Section 5:-

Summary and discussions

In this paper, a variational Doppler radar analysis system (VDRAS) was described. The basic components of VDRAS include a forward cloud model with warm rain parameterization and its adjoint. The ability of VDRAS in determining the dynamical and microphysical variables within convective storms was examined through a series of identical-twin experiments. These experiments demonstrated that detailed cloud structures in a convective storm could be retrieved by fitting the numerical model to radial velocity and rainwater data using information from dual- or single-Doppler radars. The experiments also demonstrated that the adjoint model developed by keeping the on/off switches the same as in the basic state did not cause any problem in the minimization procedure. The problems of high nonlinearity associated with some of the physical processes could be avoided by slightly modifying the schemes.It was also found that assimilating rainwater mixing ratio obtained from the reflectivity data using a $Z–q_r$ relation resulted in a better performance of the retrieval procedure compared to direct assimilation of reflectivity. When the reflectivity data in units of dBZ were directly assimilated, the nonlinearity introduced to the cost function through the highly nonlinear $Z–q_r$ relation could cause problems in the minimization procedure. Since any $Z–q_r$ relation contains approximations, we varied the constants in the $Z–q_r$ relation to test the sensitivity of the retrieval to these variations. It was shown that the retrieval was rather robust to the error caused by the change in the $Z–q_r$ relation.

When only single-Doppler information was provided, the retrieved thermal and microphysical fields were slightly degraded. Although the error in the retrieved velocity fields increased noticeably, their structures were retrieved reasonably well. If the model accurately represents the atmosphere, then the retrieval technique is quite powerful in differentiating the water vapor, cloud water, and rainwater even with observations from only one radar. However, the experiments in which the parameters of some physical processes were neglected suggested that poor representation of a moist process could have a large impact on the retrieval of the microphysical fields. Attempts to tune these parameters did not show any success with the amount of available data. Therefore, it is important to implement good physical parameterization schemes in order to obtain a reliable microphysical retrievalVDRAS was also tested on radial velocity data with a 20% random error and reflectivity data with a 3-dBZ uniform error (to mimic calibration errors), respectively. Results suggested that the technique was able to retrieve the general structure of the storm when the data contained errors at those magnitudes. However, the retrieval was more sensitive to the reflectivity calibration error than to the random noise in the radial velocity fields. In these experiments, the error statistics were not used to determine the error covariance matrix in the cost function due to the difficulty in calculating the inverse matrix. For simplicity, a constant diagonal matrix was used to approximate the error covariance matrix. In the current simulated data study, this approximation did not appear to affect the retrievalresults to a great extent. However, better approximations may be required to successfully assimilate observational data.

References:-

Armijo, L., 1969: A theory for the determination of wind and precipitation velocities with Doppler radar. *J. Atmos. Sci.,* **26,** 570–573.

Bao, J. W., and T. T. Warner, 1993: Treatment of on/off switches in the adjoint method: FDDA experiments with a simple model. *Tellus,* **45A,** 525–538.

———, and Y.-H. Kuo, 1995: On–off switches in the adjoint method: Step functions. *Mon. Wea. Rev.,* **123,** 1589–1594.

Battan, L. J., 1973: *Radar Observation of the Atmosphere.* University of Chicago Press, 324 pp.

Courtier, P., 1985: Experiments in data assimilation using the adjoint model technique. Preprints, *Workshop on High-Resolution Analysis,* Reading, United Kingdom, European Centre for Medium-Range Weather Forecasts, 1–20.

Derber, J. C., 1985: The variational 4-D assimilation of analyses using filtered models as constraints. Ph.D. dissertation, University of Wisconsin—Madison, 142 pp.

Douady, D., and O. Talagrand, 1990: The impact threshold process on variational assimilation. Preprints, *WMO Int. Symp. on Assimilation of Observations in Meteorology and Oceanography,* Clermont-Ferrand, France, World Meteor. Org., 486–487.